

# Multiplicity and centre-of-mass energy dependence of light-flavor hadron production in pp, p–Pb, and Pb–Pb collisions with ALICE

---

**Ivan Ravasenga\***, for the ALICE Collaboration

*Bogolyubov Institute for Theoretical Physics, National Academy of Science of Ukraine (Kiev)*

*E-mail:* [ivan.ravasenga@cern.ch](mailto:ivan.ravasenga@cern.ch)

In heavy-ion collisions (A–A) at the CERN Large Hadron Collider (LHC) energies, a strongly coupled Quark Gluon Plasma (QGP) is produced, giving rise to collective phenomena whose signatures can be retrieved in final state hadronic observables. Recent observations suggest the presence of collective phenomena in small systems like pp collisions. Ongoing analyses therefore try to identify whether a unified description of the pp, p–A and A–A data can be established.

The integrated yield ratios to pion yields show an increasing trend at low charged-particle multiplicity that tends to saturate at higher multiplicities. The behaviour is dependent on the strangeness content of the particle species and is totally independent of the collision system and energy (multiplicity-driven particle production). Furthermore, a blast wave analysis shows how strong radial gradients are also present in p–Pb collisions at LHC energies.

Hydrodynamic and recombination models are tested against the measured hadron spectral shapes at low and intermediate transverse momenta.

*European Physical Society Conference on High Energy Physics - EPS-HEP2019 -  
10-17 July, 2019  
Ghent, Belgium*

---

\*Speaker.

## 1. Introduction

The ALICE experiment [1] at the CERN LHC [2] has been specifically designed for the characterization of the QGP using proton-proton (pp), proton-lead (p-Pb) and lead-lead (Pb-Pb) collisions. The QGP is formed in Pb-Pb collisions while pp collisions are used as a reference. The hadrons produced in Pb-Pb collisions carry information of the evolution of the entire system. Hence, the study of the identified hadron transverse momentum ( $p_T$ ) distributions (also called spectra) gives access to measurements on flow (collective phenomena), temperature of the freeze-out phase, transverse expansion velocity of the medium and many other observables.

Combining the particle identification (PID) capabilities of the ALICE detector [1], it is possible to measure the identified hadron spectra in pp, p-Pb and Pb-Pb collisions for  $0.1 \leq p_T \leq 20$  GeV/c. In ALICE the event multiplicity is measured by means of the V0 detector (Sec. 5.4 of [1]).

Recent observations suggest the presence of collective phenomena in small systems (pp, p-Pb) [5, 3, 4]. Current research therefore aims to verify whether a unified description in terms of collective effects in pp, p-A and A-A collisions can be established [8, 7, 4].

A comparison to theoretical models [9, 17] shows how the low- $p_T$  particle production can be described by hydrodynamical models and QCD-inspired models that go beyond an incoherent superposition of parton-parton scatterings, introducing for instance color ropes [11], color reconnection [12] and core-corona effects [22].

## 2. Transverse momentum distributions

The transverse momentum distributions of identified hadrons in Pb-Pb collisions at a centre-of-mass energy per nucleon of  $\sqrt{s_{NN}} = 5.02$  TeV show a  $p_T$ -hardening as the multiplicity increases. The effect is more visible for heavier particles and it is generally attributed to the radial flow [6].

The  $p_T$ -distributions in p-Pb collisions at  $\sqrt{s_{NN}} = 8.16$  TeV for  $\pi$  and p are shown in Fig. 1 as a function of the multiplicity. From the bottom panels it is possible to clearly see the hardening of the spectra with multiplicity. In smaller systems (pp collisions) the same conclusion can be addressed in a more limited  $p_T$  range ( $p_T \leq 2$  GeV/c) suggesting the presence of radial flow effects even in small collision systems [17].

## 3. Integrated yield and average transverse momenta

The  $p_T$ -integrated yields ( $dN/dy$ ), and the average transverse momentum ( $\langle p_T \rangle$ ) for each particle species are obtained by fitting the particle spectra with specific functions extrapolating the spectra down to  $p_T = 0$  GeV/c (where no data points are measured). More details are in Refs. [7, 10, 17]. The integrated yields of several hadrons (with and without strangeness content) divided by the pion yield are shown in Fig. 2 as a function of the average charged-particle multiplicity density at mid-rapidity ( $\langle dN_{ch}/d\eta \rangle_{|\eta| < 0.5}$ ) for different colliding systems. It is possible to observe a smooth evolution of particle production with charged-particle multiplicity from pp to A-A collisions. The ratios do not depend on the centre-of-mass energy of the collisions and increase going from low to high multiplicity, indicating that the hadron chemistry is driven by the multiplicity. In addition,

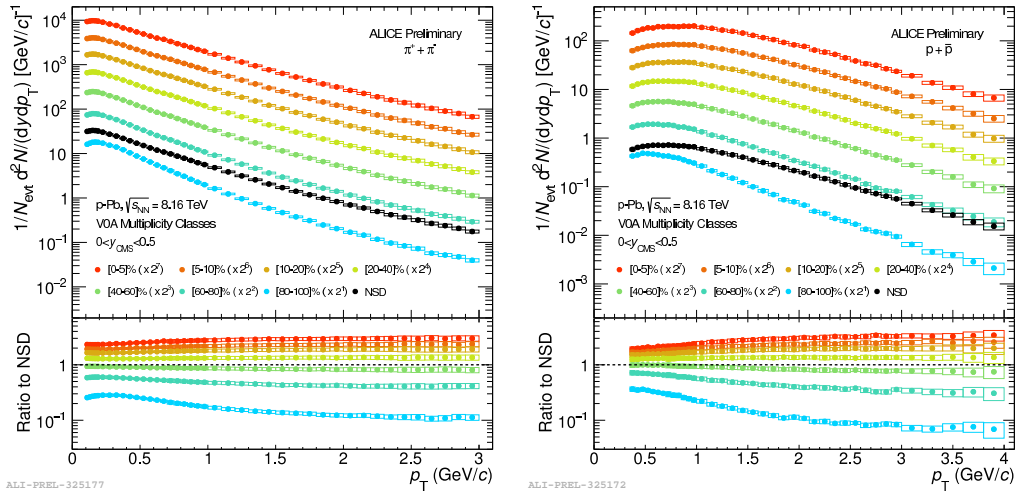


**Figure 1:** Pion and proton transverse momentum distribution in several centrality classes in p–Pb collisions at  $\sqrt{s_{NN}} = 8.16$  TeV. Boxes represent the systematic uncertainties.

the ratios increase going from low to high multiplicity events. The slope of the increase changes according to the strange-quark content of particles [15]. The increase (strangeness enhancement) is observed for small systems while a saturation is observed for larger systems. In particular the  $\phi$  meson represents a key probe for studying the strangeness production. Typically, particles with open strangeness are subject to canonical suppression in small systems (pp, p–Pb) while  $\phi$  is not. In fact the  $2\phi/\pi$  ratio shows an increasing trend for small systems that is not expected from the simple canonical suppression. This is in favour of non-equilibrium production of the  $\phi$  [17, 14].

The average transverse momenta as a function of multiplicity are shown in Fig. 3 for several

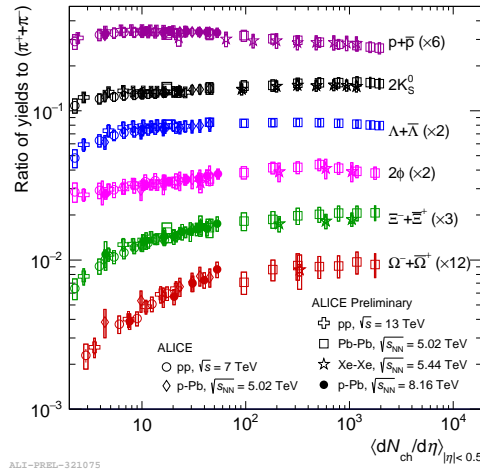


**Figure 2:** Integrated yield ratios to pion yields as a function of the charged-particle multiplicity density in several colliding systems and energies. The boxes represent the systematic uncertainties.

particle species and from small (left panel) to larger (rightmost panel) collision systems. For  $\pi$ , K and (anti-)p a mass ordering and similar trends are observed in all the systems as a function of multiplicity. The mass ordering breaks down for peripheral A–A, p–Pb and pp collisions if one

considers also the  $\phi$  meson, which has a similar mass to that of protons. In general, the moderate increase of the  $\langle p_T \rangle$  is usually attributed to increasing collective radial flow.

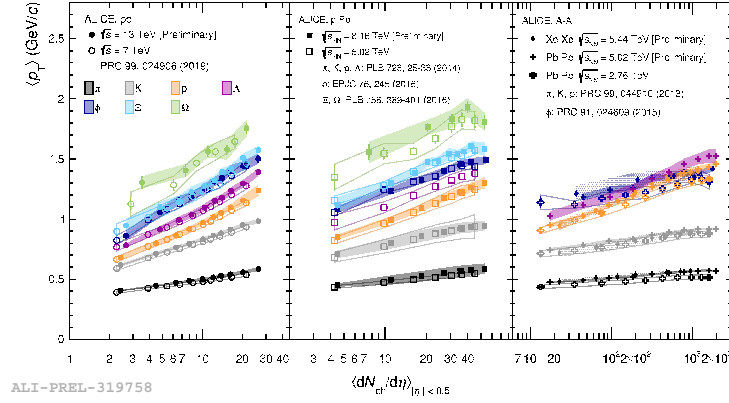


**Figure 3:** Average transverse momenta ( $\langle p_T \rangle$ ) of different particle species as a function of the charged-particle multiplicity density in several colliding systems and energies. The colliding system size increases going from the leftmost to the rightmost panel. The bands represent the systematic uncertainties.

#### 4. Blast wave analysis

The Boltzmann-Gibbs blast wave model [16] is simultaneously fitted to the pion, kaon and proton transverse momentum spectra in order to evaluate the average transverse expansion velocity distribution ( $\langle \beta_T \rangle$ ), the temperature of the kinetic freeze-out ( $T_{kin}$ ) and the exponent of the velocity profile ( $n$ ).

Figure. 4 shows the correlation between  $T_{kin}$  and  $\langle \beta_T \rangle$  for several colliding systems. The  $1\sigma$  uncertainties are shown as ellipses. It can be observed that larger  $\langle \beta_T \rangle$  are measured for Pb–Pb central collisions at  $\sqrt{s_{NN}} = 5.02$  TeV while comparable  $T_{kin}$  and  $\langle \beta_T \rangle$  are measured in Pb–Pb at different energies but at similar charged particle multiplicities. In p–Pb and Pb–Pb systems a similar trend is observed, and this is consistent with the presence of radial flow even in p–Pb collisions. At similar multiplicities, comparable  $T_{kin}$  are measured for p–Pb and Pb–Pb whereas  $\langle \beta_T \rangle$  is significantly higher in p–Pb collisions. Finally, pp and p–Pb show comparable temperatures and velocities at similar multiplicities.

#### 5. Comparison to models

The results on hadron production are compared to hydrodynamical models with different initial conditions and parametrizations of the fireball and hadronization processes. Upper panel of Fig. 5 shows a comparison of the  $\pi$ , K and p spectra to different theoretical models in central (0–5%) Pb–Pb collisions at  $\sqrt{s_{NN}} = 5.02$  TeV. In the bottom part of the plot the data-to-model ratio is computed. The comparison is done to the iEBE-VISHNU hybrid model [18] (with TRENTo [19] and AMPT [20] initial conditions), McGill [21] and EPOS-LHC [22]. As can be seen, for  $p_T < 1$  GeV/c, all the models except EPOS-LHC describe the data within 20%. EPOS-LHC fails in describing the low- $p_T$  part of the spectra because of the simple way the QGP is treated and because of the absence

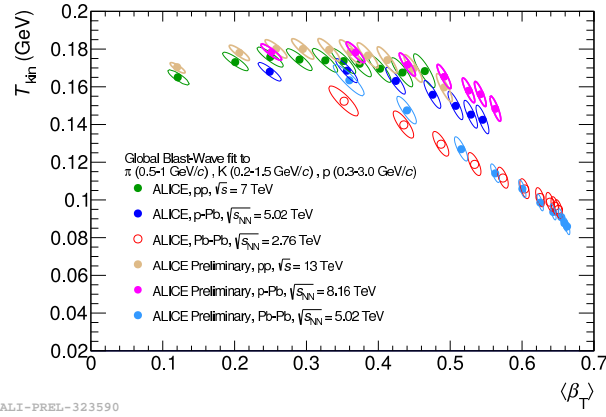


**Figure 4:** Correlation between  $T_{\text{kin}}$  and  $\langle\beta_T\rangle$  (from blast wave simultaneous fit to  $\pi$ , K and p) for different colliding systems. The ellipses represent  $1\sigma$  uncertainties.

of a hadron cascade. Instead, iEBE-VISHNU with both initial conditions can describe also the intermediate  $p_T$  region within 20%. For the same  $p_T$  regions and at higher momenta, EPOS-LHC fails to describe the data points in central (and semi-central) Pb–Pb collisions. McGill instead works well up to about  $p_T = 1.5$  GeV/c.

Finally, the lower panel of Fig. 5 shows the  $p_T$ -differential kaon-to-pion and proton-to-pion ratios compared to the same hydrodynamical models listed before in central Pb–Pb collisions. Despite some difficulties in describing the particle spectra, for  $p_T < 2$  GeV/c a good agreement between data and models is observed. In general, the K/ $\pi$  ratios are well described by all the models, while larger discrepancies are observed for p/ $\pi$  ratios where flow effects are more dominant. At intermediate  $p_T$ , where the flow peak is measured, EPOS-LHC can reproduce very well the flow effects.

## 6. Conclusions

The radial flow in Pb–Pb collisions measured with the ALICE experimental setup modifies the shape of the identified particle spectra (more evident for heavier particles) especially in central collisions. A spectral shape modification is measured also in p–Pb and pp collisions going from high multiplicity to lower multiplicity events, suggesting the presence of collective phenomena in small systems. In addition, the similarities between pp and p–Pb collisions indicate a common mechanism playing a role in these systems despite the difference in the initial state.

The integrated yield ratios to pion yields show an increase going from low to high multiplicity events with a slope that depends on the strange-quark content ( $S$ ) of particles:  $S=0$  for protons (almost flat trend), while  $S=3$  for  $\Omega$  (steep increase).

The correlation between the kinetic freeze-out temperature ( $T_{\text{kin}}$ ) and average transverse velocity ( $\langle\beta_T\rangle$ ) from blast wave analysis shows that larger  $\langle\beta_T\rangle$  are measured in p–Pb with respect to Pb–Pb collision system, while pp and p–Pb systems show similar temperatures and velocities at similar event multiplicities.

A comparison of the particle distributions to the hydrodynamical models in Pb–Pb collisions shows

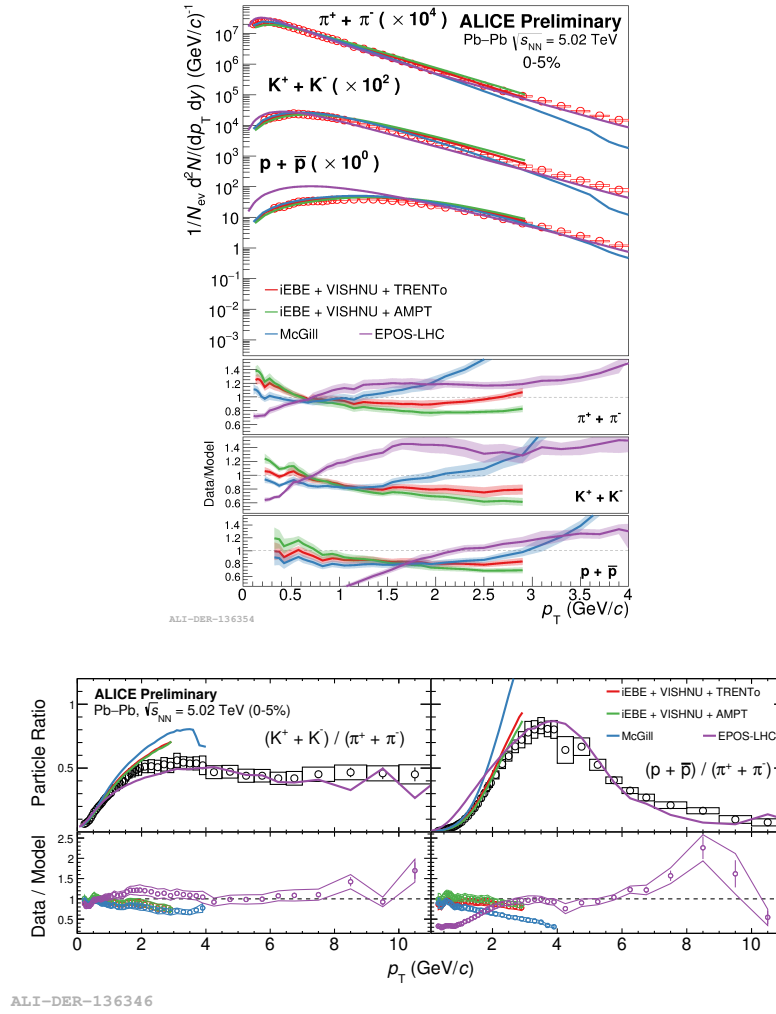


**Figure 5:** Upper panel: pion, kaon and proton  $p_T$ -spectra in 0–5% Pb–Pb collisions at  $\sqrt{s_{NN}} = 5.02$  TeV compared to hydrodynamical calculations. Lower panel: kaon-to-pion and proton-to-pion  $p_T$ -differential ratios in 0–5% Pb–Pb collisions at  $\sqrt{s_{NN}} = 5.02$  TeV compared to hydrodynamical calculations. In data/model ratios the systematic uncertainties are indicated as colored bands while the statistical ones as bars.

a data-to-model agreement within 20% for  $p_T < 1$  GeV/c. The EPOS-LHC model, instead, fails to describe the low- $p_T$  part of the distributions because of the absence of the hadron cascade model and of a fixed saturation scale. Despite the difficulties, most of the models are able to reproduce the kaon-to-pion and proton-to-pion ratios up to about  $p_T = 12$  GeV/c. In general, it is possible to conclude that the low- $p_T$  particle production is described better by hydrodynamical models which go beyond simple QCD calculations including color ropes, color reconnection and core-corona effects.

## References

- [1] ALICE Collaboration, “The ALICE experiment at the CERN LHC”, JINST 3 (2008) S08002
- [2] L. Evans, P. Bryant, “LHC Machine”, JINST 3 (2008) S08001

- [3] ALICE Collaboration, “Long-range angular correlations on the near and away side in p–Pb collisions at  $\sqrt{s_{NN}} = 5.02$  TeV”, Phys. Lett. B719 (2013) 29-41
- [4] ALICE Collaboration, “Multiplicity dependence of the average transverse momentum in pp, p–Pb, and Pb–Pb collisions at the LHC”, Phys. Lett. B727 (2013) 371-380
- [5] CMS Collaboration, “Ridge correlation structure in high multiplicity pp collisions with CMS”, J. Phys. G38 (2011) 124051
- [6] ALICE Collaboration, “Production of identified charged hadrons in Pb–Pb collisions at  $\sqrt{s_{NN}} = 5.02$  TeV”, Nucl. Phys. A967, 421 (2017)
- [7] ALICE Collaboration, “Centrality dependence of  $\pi$ , K, p production in Pb–Pb collisions at  $\sqrt{s_{NN}} = 2.76$  TeV”, Phys. Rev. C88 (2013) 044910
- [8] ALICE Collaboration, “Multiplicity Dependence of Pion, Kaon, Proton and Lambda Production in p–Pb Collisions at  $\sqrt{s_{NN}} = 5.02$  TeV”, Phys. Lett. B728 (2014) 25-38
- [9] ALICE Collaboration, “Production of charged pions, kaons and protons at large transverse momenta in pp and Pb–Pb collisions at  $\sqrt{s_{NN}} = 2.76$  TeV”, Phys. Lett. B736 (2014) 196-207
- [10] ALICE Collaboration, “Measurement of pion, kaon and proton production in proton-proton collisions at  $\sqrt{s} = 7$  TeV”, Eur. Phys. J. C75 (2015) no.5, 226
- [11] C. Bierlich et al., “Effects of Overlapping Strings in pp Collisions”, JHEP 1503 (2015) 148
- [12] T. Sjostrand, P. Z. Skands, “Transverse-momentum-ordered showers and interleaved multiple interactions”, Eur. Phys. J. C (39), 129 (2005)
- [13] T. Pierog et al., “EPOS LHC: Test of collective hadronization with data measured at the CERN Large Hadron Collider”, Phys. Rev. C92 (2015) no.3, 034906
- [14] A. K. Dash [ALICE Collaboration], “Multiplicity dependence of strangeness and hadronic resonance production in pp and p–Pb collisions with ALICE at the LHC”, Nucl. Phys. A982, 467 (2019)
- [15] ALICE Collaboration, “Enhanced production of multi-strange hadrons in high-multiplicity proton-proton collisions”, Nature Phys. 13, 535 (2017)
- [16] E. Schnedermann et al., “Thermal phenomenology of hadrons from 200 A GeV S+S collisions”, Phys. Rev. C48 (1993) 2462
- [17] ALICE Collaboration, “Multiplicity dependence of light-flavor hadron production in pp collisions at  $\sqrt{s} = 7$  TeV”, Phys. Rev. C99, no. 2, 024906 (2019)
- [18] W. Zhao et al., “Collective flow in 2.76 A TeV and 5.02 A TeV Pb+Pb collisions”, Eur. Phys. J. C77, no. 9, 645 (2017)
- [19] J. S. Moreland et al., “Alternative ansatz to wounded nucleon and binary collision scaling in high-energy nuclear collisions”, Phys. Rev. C92, no. 1, 011901 (2015)
- [20] Z. W. Lin et al., “A Multi-phase transport model for relativistic heavy ion collisions”, Phys. Rev. C72, 064901 (2005)
- [21] S. McDonald et al., “Hydrodynamic predictions for Pb+Pb collisions at 5.02 TeV”, Phys. Rev. C95, no. 6, 064913 (2017)
- [22] T. Pierog, “EPOS LHC: Test of collective hadronization with data measured at the CERN Large Hadron Collider”, Phys. Rev. C92, no. 3, 034906 (2015)